



HAL
open science

The Lactococcal Phages Tuc2009 and TP901-1 Incorporate Two Alternate Forms of Their Tail Fiber into Their Virions for Infection Specialization

Stephen R. S. R. Stockdale, Jennifer J. Mahony, Pascal P. Courtin, Marie-Pierre M.-P. Chapot-Chartier, Jan-Peter J.-P. van Pijkeren, Robert A. R. A. Britton, Horst H. Neve, Knut J. K. J. Heller, Bashir B. Aideh, Finn K. F. K. Vogensen, et al.

► To cite this version:

Stephen R. S. R. Stockdale, Jennifer J. Mahony, Pascal P. Courtin, Marie-Pierre M.-P. Chapot-Chartier, Jan-Peter J.-P. van Pijkeren, et al.. The Lactococcal Phages Tuc2009 and TP901-1 Incorporate Two Alternate Forms of Their Tail Fiber into Their Virions for Infection Specialization. *Journal of Biological Chemistry*, 2013, 288 (8), pp.5581 - 5590. 10.1074/jbc.M112.444901 . hal-01001577

HAL Id: hal-01001577

<https://hal.science/hal-01001577>

Submitted on 29 May 2020

HAL is a multi-disciplinary open access archive for the deposit and dissemination of scientific research documents, whether they are published or not. The documents may come from teaching and research institutions in France or abroad, or from public or private research centers.

L'archive ouverte pluridisciplinaire **HAL**, est destinée au dépôt et à la diffusion de documents scientifiques de niveau recherche, publiés ou non, émanant des établissements d'enseignement et de recherche français ou étrangers, des laboratoires publics ou privés.

Copyright

The Lactococcal Phages Tuc2009 and TP901-1 Incorporate Two Alternate Forms of Their Tail Fiber into Their Virions for Infection Specialization^{*S}

Received for publication, December 14, 2012, and in revised form, January 7, 2013. Published, JBC Papers in Press, January 8, 2013, DOI 10.1074/jbc.M112.444901

Stephen R. Stockdale[‡], Jennifer Mahony[‡], Pascal Courtin^{S¶}, Marie-Pierre Chapot-Chartier^{S¶}, Jan-Peter van Pijkeren^{||}, Robert A. Britton^{||}, Horst Neve^{**}, Knut J. Heller^{**}, Bashir Aideh^{††}, Finn K. Vogensen^{††}, and Douwe van Sinderen^{‡S§1}

From the [‡]Department of Microbiology and ^{S§}Alimentary Pharmabiotic Centre, University College Cork, Cork, Ireland, ^SINRA, UMR1319 Micalis, Jouy-en-Josas, France, [¶]AgroParisTech, UMR Micalis, Jouy-en-Josas, France, the ^{||}Department of Microbiology and Molecular Genetics, Michigan State University, East Lansing, Michigan 48824, the ^{**}Department of Microbiology and Biotechnology, Max Rubner-Institut, Kiel, Germany, and the Department of Food Science, ^{††}University of Copenhagen, Copenhagen, Denmark

Background: Siphoviridae virions often possess lytic domains facilitating host-penetration.

Results: Tuc2009 and TP901-1 virions may contain full-length or truncated tail fibers, possessing or lacking a lytic domain, respectively.

Conclusion: Phages with a lytic domain infect stationary phase cells better, whereas truncated derivatives have higher adsorption efficiencies.

Significance: The heterogeneous phage population serves to most effectively infect bacteria where levels of cell wall cross-linkage differ.

Lactococcal phages Tuc2009 and TP901-1 possess a conserved tail fiber called a tail-associated lysin (referred to as Tal₂₀₀₉ for Tuc2009, and Tal₉₀₁₋₁ for TP901-1), suspended from their tail tips that projects a peptidoglycan hydrolase domain toward a potential host bacterium. Tal₂₀₀₉ and Tal₉₀₁₋₁ can undergo proteolytic processing mid-protein at the glycine-rich sequence GG(S/N)SGGG, removing their C-terminal structural lysin. In this study, we show that the peptidoglycan hydrolase of these Tal proteins is an M23 peptidase that exhibits D-Ala-D-Asp endopeptidase activity and that this activity is required for efficient infection of stationary phase cells. Interestingly, the observed proteolytic processing of Tal₂₀₀₉ and Tal₉₀₁₋₁ facilitates increased host adsorption efficiencies of the resulting phages. This represents, to the best of our knowledge, the first example of tail fiber proteolytic processing that results in a heterogeneous population of two phage types. Phages that possess a full-length tail fiber, or a truncated derivative, are better adapted to efficiently infect cells with an extensively cross-linked cell wall or infect with increased host-adsorption efficiencies, respectively.

It is predicted that 60% of the estimated 10³¹ phages in the biosphere belong to the Siphoviridae (1, 2). Yet despite their prevalence, the molecular details surrounding the initiation of infection by such siphophages are not fully resolved. The Siphoviridae tail tip is a multiproteinaceous structure responsible for host recognition and the initiation of phage infection. Siphoviridae often possess a central tail fiber suspending from their tail tip known to be essential for various aspects of phage infection such as tail morphogenesis, bacterial adsorption, cell envelope penetration, and directing DNA ejection (3–11).

Coliphages λ and T5 and *Bacillus* phage SPP1 are arguably the best studied models for understanding the various roles that central tail fiber proteins fulfill during Siphoviridae infection. λ possesses a central tail fiber, composed of three copies of gpJ protein, which forms a hub around which the tail organelle assembles (3). The C terminus of gpJ functions as a receptor-binding protein, attaching to LamB on the surface of *Escherichia coli* (5, 12). The tail tube tips of reversibly bound λ particles are ~17 nm from the cell surface, whereas the tail tube tips are in direct contact with the bacterial envelope when this phage is irreversibly bound to its host (13). The transition from reversibly to irreversibly bound phage λ coincides with conformational changes in gpJ (detected through proteinase sensitivity) and the appearance of a transmembrane channel proposed to be formed by the tape measure protein (TMP)² gpH (10, 14).

The tail protein Pb2 of Siphoviridae phage T5 serves both as the TMP and straight tail fiber. Insertion of purified Pb2 into black lipid membranes results in the formation of pores of ~2-nm diameter (15). The C terminus of Pb2 possesses a PGH domain, which promotes the penetration of the *E. coli* cell envelope (9). Located between the TMP and tail fiber region domains of Pb2 are two transmembrane domains. These have been shown to insert the tail fiber of T5 into a lipid layer containing the proteinaceous receptor, FhuA, of T5. Insertion of Pb2 into FhuA-containing liposomes causes conformational

* This work was supported by Institut National de la Recherche Agronomique (INRA), Région Ile de France, and Agence Nationale Recherche (ANR) French National Research Agency (ANR Lacto-Phages).

^S This article contains supplemental Tables 1 and 2.

¹ A recipient of a Science Foundation Ireland Principal Investigatorship award (Ref. No. 08/IN.1/B1909). To whom correspondence should be addressed: Dept. of Microbiology and Alimentary Pharmabiotic Centre, University College Cork, Ireland. Tel.: 353-21-4901365; E-mail: d.vansinderen@ucc.ie.

² The abbreviations used are: TMP, tape measure protein; PGH, peptidoglycan hydrolase; COI, center of infection; ECOI, efficiency of COI.

Tail-associated Lytic Enzymes of Siphoviridae Phages

TABLE 1
Bacteria, phage, and plasmids used in this study

Strains, phages, and plasmids	Relevant features	Source
<i>L. lactis</i>		
MG1363	Prototypical <i>L. lactis</i> strain	Ref. 58
NZ9000	MG1363 <i>pepN::nisRK</i>	Ref. 36
901-1erm	Lysogenic host and source of TP901-1erm prophage	Refs. 59 and 60
3107	Lytic host for phage TP901-1erm	Ref. 52
UC509	Lysogenic host and source of Tuc2009 prophage	Ref. 35
UC509.9	Lytic host for phage Tuc2009	Ref. 62
NZ9700	Nisin overproducing strain	Ref. 63
NZ9000-TP901-1erm	NZ9000 lysogenized with TP901-1erm prophage	This study
NZ9000-TP901-1erm _{Gly>Arg}	Glycine to arginine mutations in the proteolysis site of TP901-1erm prophage Tal ₉₀₁₋₁ protein	This study
NZ9000-TP901-1erm _{H892A}	Histidine to alanine mutation at amino acid position 892 of TP901-1erm prophage Tal ₉₀₁₋₁ protein	This study
NZ9000-TP901-1erm _{Gly603*}	Stop codon inserted in TP901-1 prophage Tal ₉₀₁₋₁ proteolysis site sequence mimicking natural truncation	This study
Phage		
TP901-1erm	Temperate P335 species phage infecting 3107; contains erythromycin marker	Refs. 59 and 60
Tuc2009	Temperate P335 species phage infecting UC509.9	Ref. 62
TP901-1erm _{Gly>Arg}	TP901-1 phage with glycine to arginine mutations in the proteolysis site of Tal ₉₀₁₋₁ protein	This study
TP901-1erm _{H892A}	TP901-1 phage with Tal ₉₀₁₋₁ histidine at position 892 mutated to alanine	This study
TP901-1erm _{Gly603*}	TP901-1 phage with stop codon inserted at the site of Tal ₉₀₁₋₁ proteolysis	This study
Plasmid		
pNZ8048	Nisin-inducible protein expression vector	Ref. 61
pQE60	QIAGEN expression vector, N-terminal His ₆ tag	Qiagen
pREP4	QIAGEN vector supplying LacI	Qiagen
pJP005	pNZ8048 derivative expressing RecT protein	Ref. 32
pNZ9530	Nisin helper plasmid supplying NisRK genes for protein expression; erythromycin marker	Ref. 16
pTalM23-LysM	pNZ8048 construct expressing TalM23-LysM recombinant protein	This study
pTal ₂₀₀₉ -5ΔN	pQE60 construct expressing terminal 501 bp of Tal ₂₀₀₉	Ref. 31
pTal ₉₀₁₋₁ -5ΔN	pQE60 construct expressing terminal 501 bp of Tal ₉₀₁₋₁	This study
pTal ₉₀₁₋₁ -5ΔN _{H892A}	pQE60 construct expressing terminal 501 bp of Tal ₉₀₁₋₁ from mutant TP901-1erm _{H892A}	This study

changes in Pb2, shortening its length while simultaneously doubling its width from 2 to 4 nm (9, 17).

The central tail fiber of *Bacillus subtilis* phage SPP1 is composed of three copies of gp21 (11). The N terminus of gp21 forms a cap at the distal end of the tail tube, which has been shown to open at the onset of infection (18). The C terminus of gp21 acts as a receptor binding protein attaching to the membrane-spanning protein YueB (19–21). Irreversible adsorption of SPP1 to YueB initiates infection and is accompanied by conformational changes transmitted across the full-length of the tail tube to the portal protein by means of a cascading rotational movement of the major tail protein of the siphophage (11).

Siphoviridae phages infecting lactic acid bacteria, and in particular *Lactococcus lactis*, are the single largest cause of industrial milk fermentation problems and result in significant economic losses (22). The P335 phage species is one of the three major lactococcal infecting phage species that cause regular problems for the dairy industry (the other species being c2 and 936) (23, 24). Scientific efforts to understand and control this particular problem in the dairy industry have allowed lactococcal phages to become one of the most intensely studied phage groups and one of the model systems for understanding how Siphoviridae phages infect their host (25).

The tail fiber of lactococcal phages Tuc2009 and TP901-1 is composed of a trimer of the so-called Tal protein, which between them share 95% amino acid identity (26). Tal₂₀₀₉ and Tal₉₀₁₋₁ are predicted to possess a C-terminally located M23 peptidase PGH domain, which distally protrudes from the large host-recognizing baseplate structure of each of these phages (27–29). The N terminus of Tal₂₀₀₉ and that of Tal₉₀₁₋₁ both share 26% amino acid identity with the N terminus of SPP1 tail fiber protein gp21 (30). The N-terminal portion of Tal₂₀₀₉ and Tal₉₀₁₋₁ is therefore expected to fulfill an analogous role at the initiation of infection, opening to facilitate ejection of the TMP

and DNA. Located between the predicted C-terminal M23 peptidase domain and the N-terminal tail tube cap of Tal₂₀₀₉ and Tal₉₀₁₋₁ is a glycine-rich sequence, GG(S/N)SGG. Interestingly, GGSSG*GG has been shown to undergo proteolysis *in vitro* and *in vivo* (cleavage location indicated by an asterisk), which results in mature Tuc2009 virions that have incorporated both full-length and truncated Tal proteins (31).

Here, we present the biochemical and mutational analysis of Tal to further understand the role of tail fiber proteins during infection. The importance of the cell wall-degrading activity and proteolytic processing of Tal₂₀₀₉ and Tal₉₀₁₋₁ for host penetration and adsorption is discussed and placed within the context of current knowledge on host penetration by Siphoviridae phages.

MATERIALS AND METHODS

Bioinformatic Analysis—Relevant DNA sequences were downloaded from NCBI and manipulated using the DNASTAR software package (DNASTAR, Inc., Madison, WI). Protein domains were identified using InterProScan from EMBL-EBI. Multiple sequence alignments were generated online using the ClustalW program (EMBL). The amino acid percentage identity between protein sequences was estimated by BLAST2p (<http://blast.ncbi.nlm.nih.gov/Blast.cgi>).

Bacterial Strains, Culture Conditions, Phage Preparations, and Plasmids—Bacteria, phages, and plasmids used in this study are listed in Table 1. *L. lactis* strains were grown at 30 °C in M17 (Oxoid) broth or agar supplemented with 0.5% (w/v) glucose (GM17). Erythromycin and chloramphenicol were used as necessary at concentrations of 5 and 10 μg/ml, respectively. *L. lactis* strain NZ9000 carrying the TP901-1erm prophage was isolated by simultaneously inoculating 2% (v/v) NZ9000 from a fresh overnight and 2% (v/v) TP901-1erm from a 10¹⁰ PEG-precipitated lysate, followed by a 6-h incubation,

before selecting for erythromycin-resistant colonies. Large-scale phage preparations of TP901-1*erm* and mutant derivatives were performed as described previously (4) by inducing 1.6 L of the lysogenized NZ9000 host with mitomycin C. TBT buffer (100 mM NaCl, 50 mM CaCl₂, 10 mM MgCl₂, 20 mM Tris-HCl (pH 7.0)) was used as the phage resuspension buffer.

Recombineering and Oligonucleotides—All oligonucleotides used in this study are shown in supplemental Table 1. Recombineering was performed as described previously (32). However, specific modifications optimized for *L. lactis* such as phosphorothioate linkages and transforming 500 μg of oligonucleotides were also employed (33). Recombineering oligonucleotides were ordered from Integrated DNA Technologies (Leuven, Belgium), whereas all other oligonucleotides were ordered from Eurofins MWG (Ebersberg, Germany).

Protein Expression and Purification—The terminal 501 bp of the 3'-end of *tal*₂₀₀₉, was overproduced in *E. coli* using the pQE60 vector construct named pTal₂₀₀₉-5ΔN as described previously (31). The 501-bp 3'-end of *tal*₂₀₀₉ was also used to fuse it in-frame with the DNA encoding two LysM cell wall-binding domains of the endolysin of Tuc2009 by Splicing by Overlap Extension (SOEing) PCR (34, 35). The resulting amplicon, which specified a Tal₂₀₀₉M23peptidase-LysM fusion protein and designated TalM23-LysM, was cloned into pNZ8048 using standard techniques, to generate plasmid pTalM23-LysM. The TalM23-LysM protein was overproduced in NZ9000 using the NICE expression system (36) and required purification using a denaturing renaturation procedure as described in the QIAexpressionist handbook (Qiagen).

The terminal 501-bp regions of the tail fiber of TP901-1, amplified using TP901-1*erm* and mutant TP901-1*erm*_{H892A} lysates as DNA templates, were cloned into pQE60 as described for pTal₂₀₀₉-5ΔN, and the corresponding proteins, named Tal₉₀₁₋₁-5ΔN and Tal₉₀₁₋₁-5ΔN_{H892A}, respectively, were overproduced and purified as described above.

Assay for Lytic Activity—*L. lactis* UC509.9 cells were autoclaved, and the insoluble material was washed twice with water, once with 10 mM sodium phosphate buffer (pH 6.5), and finally resuspended in the latter buffer to produce a suspension with an *A*₆₀₀ of 0.450. All lysis experiments were performed in triplicate at 30 °C. Although only water was added to the negative control, mutanolysin (Sigma), at a concentration of 0.1 units/ml, was used in all samples to hydrolyze the glycan strand linkages of the lactococcal cell wall. Tal₂₀₀₉-5ΔN and TalM23-LysM were added at 1.0 and 1.7 μg/ml (equimolar concentrations), respectively, to achieve further degradation of the cell wall. This combined degradation of the cell wall results in lysis and in a reduction in *A*₆₀₀. Cell wall hydrolysis using Tal₉₀₁₋₁-5ΔN and Tal₉₀₁₋₁-5ΔN_{H892A} was performed in a similar manner, except that autoclaved cells were prepared from the TP901-1 host *L. lactis* 3107. Tal₉₀₁₋₁-5ΔN and Tal₉₀₁₋₁-5ΔN_{H892A} were assayed at equal concentrations of 1.75 μg/ml.

Determination of Hydrolytic Specificity on Pure Peptidoglycan (PG)—*L. lactis* MG1363 PG was prepared and hydrolyzed by mutanolysin as described previously (37). The resulting soluble muropeptides were reduced with sodium borohydride. Following this predigestion step and prior to the addition of TalM23-LysM, the samples were adjusted to pH 6.5 by the

addition of NaOH. TalM23-LysM-mediated digestion of MG1363 PG-derived muropeptides was carried out for 16 h at 30 °C with gentle agitation, using 0.04 mg/ml of enzyme. Samples were then analyzed by reverse phase HPLC with an Agilent UHPLC1290 system using ammonium phosphate buffer and methanol linear gradient as described previously (34). All of the peaks of the mutanolysin digest and most of the peaks (peaks 4 to 12) of the mutanolysin plus TalM23-LysM digest were analyzed without desalting by MALDI-TOF MS using a Voyager-DE STR mass spectrometer (Applied Biosystems) as reported previously (37). Structural identification of the muropeptides was deduced from the previously published reference profile (37).

Phage Assays—Phages used in this study were induced from their lysogenic host by the addition of 3 μg/ml mitomycin C (Sigma) to a liquid culture of the relevant strain when it had reached an *A*₆₀₀ of 0.1. Phage lysates were sterilized by filtration (0.45-μm pore filter) and stored at 4 °C. Phage titers were determined in triplicate by plaque assay employing three independent lysates using the standard double agar method (38) against the TP901-1 sensitive host *L. lactis* 3107. All GM17 media contained 5 g/liter glycine and 10 mM CaCl₂.

Adsorption assays were performed against host 3107 at an *A*₆₀₀ of 0.3 with a phage host multiplicity of infection of 0.01. Phages were allowed to adsorb for 10 min at 30 °C in the presence of 10 mM CaCl₂. The adsorption assay control without bacterial cells (*i.e.* medium only) allowed enumeration of the initial phage titer. The percentage of phage that adsorbed was calculated as ((initial phage titer – final phage titer)/initial phage titer) × 100 (39).

To compare the ability of TP901-1 and its Tal protein mutant derivatives to infect exponential phase or stationary phase cultures, center of infection (COI) assays were performed. Phage infection of *L. lactis* 3107 was performed using a multiplicity of infection of 0.01 at 30 °C in the presence of 10 mM CaCl₂. Phages were added to exponentially growing 3107 strain at *A*₆₀₀ ~ 0.3 (host 1) or to stationary phase cells of 3107 following culture dilution to *A*₆₀₀ ~ 0.3 using cell-free “spent” GM17 medium (host 2). After 10 min, cells were washed twice in GM17 to remove free phage, and subsequent dilutions were plaque assayed against an uninfected 3107 culture to determine the COI values of host 1 and host 2, after which the efficiency of COI (ECOI) formation was calculated as ((COI_{host 1})/(COI_{host 2})) (40).

Competition assays between Tal₉₀₁₋₁ mutants TP901-1*erm*_{Gly>Arg}, which possesses a full-length tail fiber, and TP901-1*erm*_{Gly603}^{*}, which has a truncated Tal protein, were performed to directly compare the biological significance of the tail fiber and associated lytic domain. An equal volume of freshly prepared phage lysates of TP901-1*erm*_{Gly>Arg} and TP901-1*erm*_{Gly603}^{*} were mixed together, and the phage mixture was diluted 1:10 into both an exponential and stationary phase culture of *L. lactis* 3107 as described above, except the phages were allowed only 5 min to establish infection.

Western Blots—Phage proteins, from CsCl-purified phage particles, were separated on a pre-cast 12% SDS-PAGE gel (Thermo Scientific) using a 0.1 M Tris-HCl, 0.1 M HEPES, 3.0 mM SDS (pH 8.0) running buffer. Proteins were transferred to a

Tail-associated Lytic Enzymes of Siphoviridae Phages

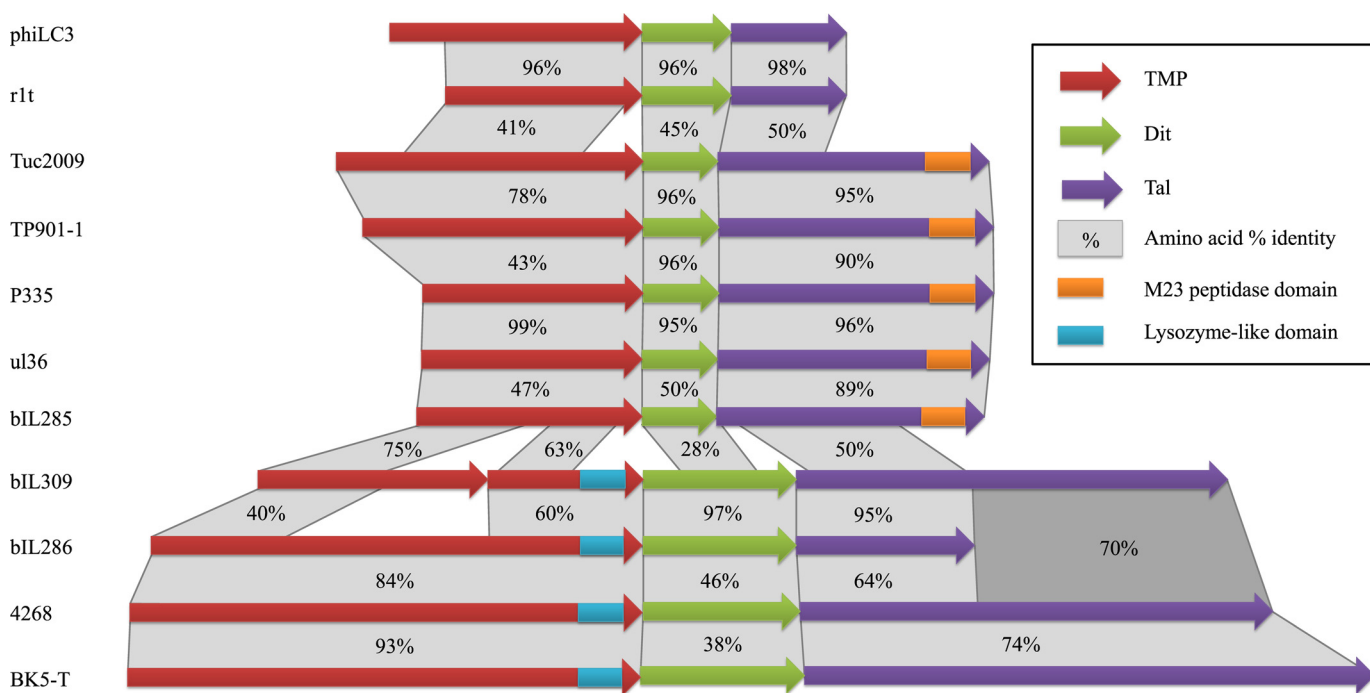


FIGURE 1. **Comparative analysis of the TMP, Dit, and Tal proteins from P335 species phages.** The locations of predicted peptidoglycan hydrolase domains are highlighted by colored boxes, as indicated in the legend. The percentage amino acid identity between protein sequences was estimated by BLAST2p and is indicated in the shaded gray boxes.

nitrocellulose membrane (Hybond-C Extra, Amersham Biosciences) in an electrotransfer unit (Bio-Rad) for 2 h at 100 V, in a 10% methanol, 10 mM 3-(cyclohexylamino)-1-propanesulfonic acid (CAPS; pH 11.0) transfer buffer, which was kept cool by placing the unit on ice. The two primary antibodies for Western blots, recognizing the N terminus of the Tal protein or the baseplate protein BppU, had been described previously (41) and shown to interact with the relevant protein of both Tuc2009 and TP901-1 (4). Western blot secondary antibodies, IRDye 680RD goat anti-rabbit antibodies (Li-Cor Biosciences), and prestained protein molecular weight ladder (11–250 kDa; Li-Cor Biosciences) were detected in the 700-nm channel using an Odyssey CLx infrared imager (Li-Cor Biosciences).

RESULTS

Analyses of P335 Species Structural Proteins to Identify Virion-associated PGH Domains—Kenny and colleagues (31) previously demonstrated that the P335 species phage Tuc2009 possesses a tail-associated lytic activity. Analysis of the genomes of two c2-type and forty 936-type phages did not reveal PGH domains associated with tail proteins (data not shown). The genomes of the eleven publicly available P335 species phages (23) all contain a gene that encodes an easily recognizable (due to its large size) TMP, followed by two genes that specify the Dit (distal tail protein) and tail fiber protein (see Fig. 1) (25). ClustalW alignments of the presumed TMP, Dit, and tail fiber protein sequences resulted in four closely related P335 species phage with a lysozyme-like domain associated with their TMP, five closely related P335 species phages with M23 peptidase domains associated with their tail fiber proteins, and two P335 species phage with no recognizable PGH domain (Fig. 1).

Tal₂₀₀₉ PGH Activity against Lactococcal Cells—The constructs Tal₂₀₀₉-5ΔN and TalM23-LysM both generate proteins with the same the C-terminal M23 peptidase of Tal₂₀₀₉ tail fiber; however, the latter contains two additional LysM cell wall binding domains (Fig. 2A). To verify the cell wall-degrading activity of Tal₂₀₀₉-5ΔN and TalM23-LysM proteins, the lytic activity of these purified recombinant enzymes was assayed on autoclaved bacterial cells as outlined under “Material and Methods.” Neither the addition of water (negative control) nor the addition of mutanolysin at low concentrations (0.1 units/ml) resulted in significant lysis of autoclaved cells, as measured through A₆₀₀ reduction of the PG-containing suspension (Fig. 2B). In contrast, a combination of mutanolysin plus Tal₂₀₀₉-5ΔN or TalM23-LysM resulted in a clear reduction in A₆₀₀. TalM23-LysM was significantly more effective at hydrolyzing PG relative to Tal₂₀₀₉-5ΔN >20 h (Fig. 2B), which is consistent with other reports where the addition of cell wall binding motifs were used to increase the lytic activity of PGH catalytic domains (42–44). TalM23-LysM was therefore used in subsequent analyses.

Characterization of Tal₂₀₀₉ PGH Hydrolytic Specificity—The PGH catalytic domain of Tal₂₀₀₉ is located at its C-terminal extremity, as reported previously and confirmed here, and contains an M23 peptidase domain (31). The M23 peptidase family includes endopeptidases that target the interpeptide bridge of PG. To confirm this prediction, it was necessary to identify the specific chemical bond targeted by the purified TalM23-LysM. PG was extracted from *L. lactis* MG1363 and first degraded by mutanolysin, a muramidase, as described previously by Courtin *et al.* (37). The resulting soluble muropeptides were further incubated with the TalM23-LysM recombinant protein. Muro-

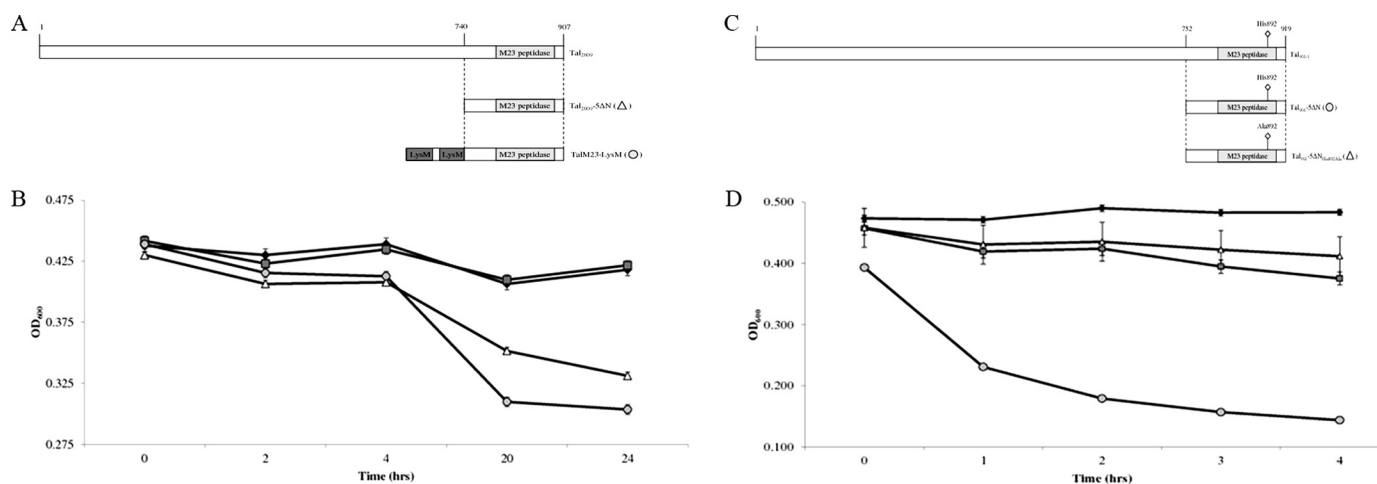


FIGURE 2. Analysis of peptidoglycan hydrolase activity associated with M23 peptidase of Tal protein constructs. *A*, diagrammatic representation of Tal₂₀₀₉ tail fiber and recombinant proteins Tal₂₀₀₉-5ΔN and TalM23-LysM. *B*, hydrolysis of *L. lactis* UC509.9 cell wall. The negative control (water) is marked as *black diamonds*, mutanolysin-only is marked with *dark gray squares*, mutanolysin and Tal₂₀₀₉-5ΔN is marked with *white triangles*, and mutanolysin and TalM23-LysM are marked with *light gray circles*. Error bars indicate S.D., whereas *asterisks* are located above statistically significant values ($p < 0.001$). *C*, diagram displaying Tal₉₀₁₋₁ tail fiber and recombinant proteins Tal₉₀₁₋₁-5ΔN and Tal₉₀₁₋₁-5ΔN_{H892A}. The histidine or alanine amino acid at position 892 in the M23 peptidase catalytic site of constructs Tal₉₀₁₋₁-5ΔN and Tal₉₀₁₋₁-5ΔN_{H892A}, respectively, is highlighted. *D*, hydrolysis of *L. lactis* 3107 cell wall. The negative control (water) is marked as *black diamonds*, mutanolysin-only is marked with *dark gray squares*, mutanolysin and Tal₉₀₁₋₁-5ΔN is marked with *white triangles*, and mutanolysin and Tal₉₀₁₋₁-5ΔN_{H892A} is marked with *light gray circles*. Error bars indicate S.D., whereas *asterisks* are located above statistically significant values ($p < 0.001$).

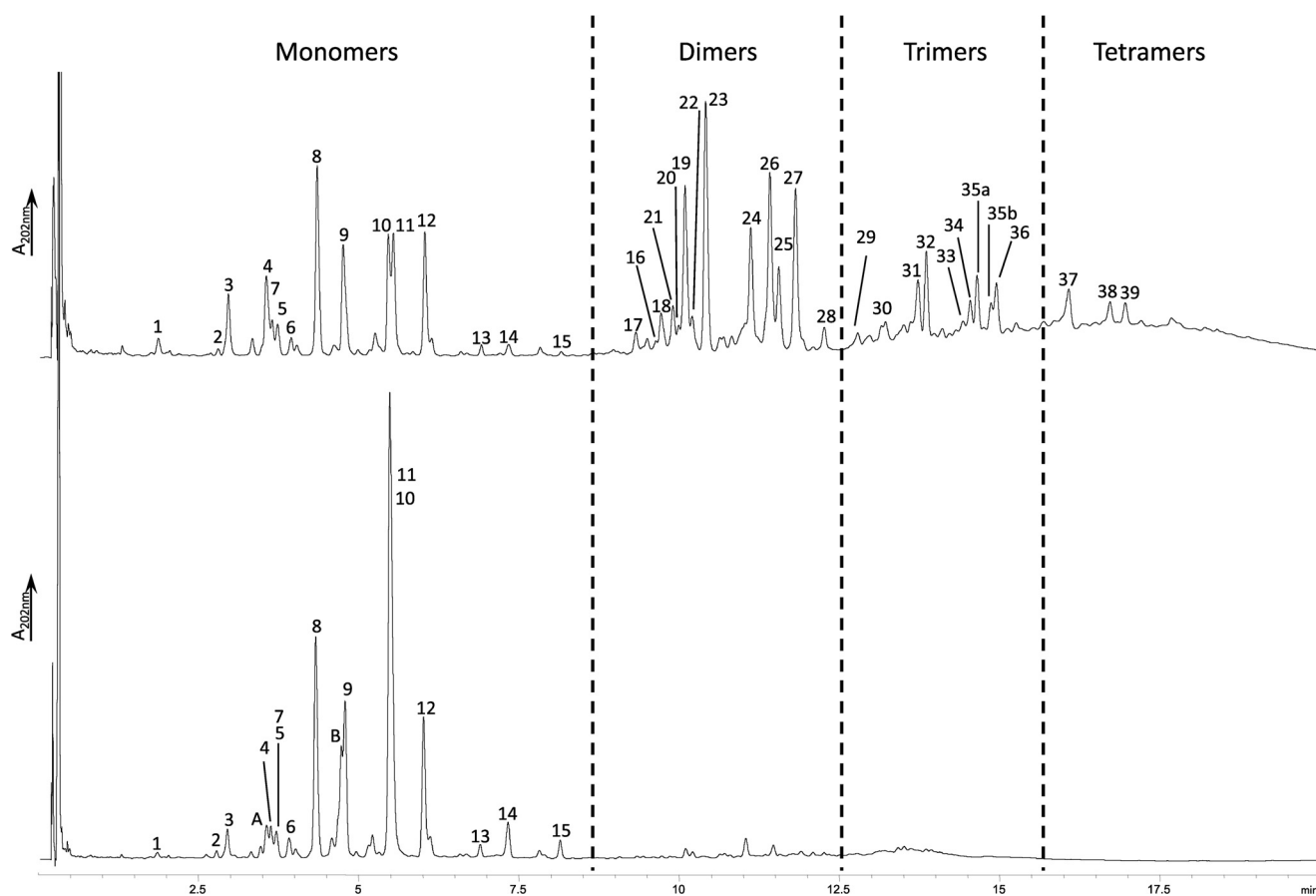


FIGURE 3. Reverse phase HPLC separation of muropeptides obtained by digestion of *L. lactis* PG by mutanolysin (A) and mutanolysin + TalM23-LysM (B). Peak numbers refer to structures identified by MALDI-TOF (supplemental Table 2).

peptides obtained after mutanolysin digestion (Fig. 3A) and after mutanolysin plus TalM23-LysM digestion (Fig. 3B) were separated by reverse phase HPLC. Comparison of the two obtained profiles revealed that the higher molecular weight

muropeptides obtained by mutanolysin digestion of PG such as dimers (peaks 16–30), trimers (peaks 31–36), and tetramers (peaks 37–39) were degraded by TalM23-LysM to its constituent monomers (peaks 1–15; see supplemental Table 2). This

Tail-associated Lytic Enzymes of Siphoviridae Phages

pattern of degradation shows that the PGH catalytic domain of Tal₂₀₀₉ acts as an endopeptidase that hydrolyzes the lactococcal peptidoglycan within the interpeptide bridge at the D-Ala-D-Asp/Asn bond. Thus, similar to other M23 peptidases (45–47), Tal₂₀₀₉ is a D,D-endopeptidase able to hydrolyze PG cross-bridges.

Construction of NZ9000-TP901-1erm for Tal₉₀₁₋₁ Mutagenesis—To investigate the precise role of lactococcal Tal proteins during infection, mutagenesis was attempted on the gene encoding the Tal₂₀₀₉ protein. However, no mutagenesis system was found to be compatible with the host strain UC509.9 of Tuc2009 (results not shown). As Tal₂₀₀₉ and Tal₉₀₁₋₁ share 95% amino acid identity, and because mutagenesis of the TP901-1 genome has been reported previously (4, 48–50), mutagenesis was instead performed on the Tal₉₀₁₋₁ genome. However, rather than using the rather laborious pGhost mutagenesis method (51), we decided to employ recombineering, a mutagenesis system that has recently been adopted for *L. lactis* (32, 33).

For the purpose of achieving TP901-1 mutagenesis by recombineering, we constructed a derivative of *L. lactis* strain NZ9000 that harbored the TP901-1erm prophage (a derivative of TP901-1 carrying an erythromycin marker; (50)), which was designated NZ9000-TP901-1erm (see “Materials and Methods”). The integration of TP901-1erm via attB-attP recombination (52) was confirmed by (a) the lack of a PCR product with primers, which flanked NZ9000s attB sequence, and (b) by generating PCR products from the primers flanking the NZ9000 attB sequence to TP901-1 chromosomal sequences (results not shown). TP901-1erm phages induced from NZ9000 with mitomycin C were still capable of infecting *L. lactis* 3107 at levels of ~10⁷ pfu/ml.

Employing the NZ9000-TP901-1erm strain, we introduced three different mutations in the tal₉₀₁₋₁ gene, which resulted in three mutant TP901-1erm phages, designated TP901-1erm_{Gly>Arg}, TP901-1erm_{H892A} and TP901-1erm_{Gly603*}, and discussed in detail below.

Characterization of Tal₉₀₁₋₁ Mutants—Specific mutations were made in TP901-1 Tal protein to investigate the role(s) of the various conserved features observed in Tal₂₀₀₉ and Tal₉₀₁₋₁ during infection. Mutant TP901-1erm_{Gly>Arg} was based on previous work (31), which had shown that altering the DNA sequence of three glycine codons, corresponding to the proteolytic processing site GGSSGGG of Tal₂₀₀₉, to arginine codons, GRSSRRG, prevented *in vitro* proteolysis. The desired mutation was introduced into the TP901-1erm genome, and one such mutant prophage was selected, and its genome was sequenced to verify the genotype of the generated mutant phage. Western blots detecting the N terminus of Tal₉₀₁₋₁ protein verified that the mutated Tal protein of mutant TP901-1erm_{Gly>Arg} was unable to undergo proteolysis as only a single band corresponding to the full-length Tal₉₀₁₋₁ protein (102.1 kDa) was detected, in contrast to the Tal protein of TP901-1erm (Fig. 4).

The second mutation in tal₉₀₁₋₁, generating mutant prophage TP901-1erm_{H892A}, was designed to inactivate the M23 peptidase domain, as demonstrated for the *Bacillus subtilis* prophage SP-β (45). The histidine at position 892 (His-892) of

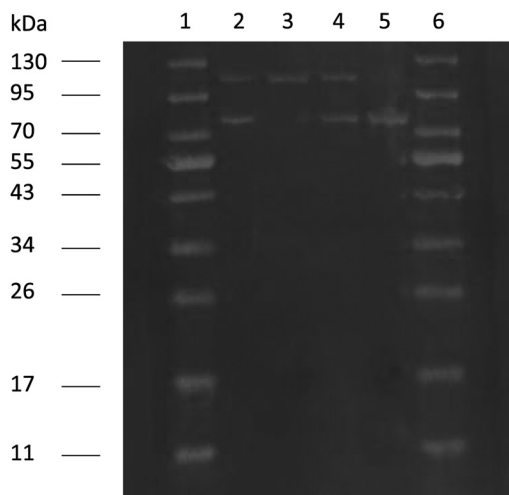


FIGURE 4. Western blots of TP901-1erm and mutant derivatives using anti-N-terminal Tal₂₀₀₉ antibodies. Lanes 1 and 6, molecular weight ladder; lanes 2–5, TP901-1erm, TP901-1_{Gly>Arg}, TP901-1_{H892A}, and TP901-1_{Gly603*}, respectively.

Tal₉₀₁₋₁, underlined in the M23 peptidase sequence PHLLHF of TP901-1erm, was targeted for mutation to an alanine residue as this is the first histidine in the HxH motif characteristic of zinc metallopeptidases (53). To verify that the M23 peptidase of mutant TP901-1erm_{H892A} was inactive, recombinant proteins of the C-terminal M23 peptidase domain of TP901-1 were created. Constructs Tal₉₀₁₋₁-5ΔN and Tal₉₀₁₋₁-5ΔN_{H892A}, representing the same C-terminal regions of their respective tail fibers as construct Tal₂₀₀₉-5ΔN, were assayed against auto-claved cells of *L. lactis* 3107 (see Fig. 2C). As expected, recombinant enzyme Tal₉₀₁₋₁-5ΔN derived from TP901-1erm showed lytic activity, whereas Tal₉₀₁₋₁-5ΔN_{H892A}, constructed from mutant TP901-1erm_{H892A}, showed no activity (see Fig. 2D). Western blots determined that the Tal protein of mutant TP901-1_{H892A} still undergoes proteolytic processing. This is evident as the full-length and truncated Tal₉₀₁₋₁ proteins (102.1 and 67.4 kDa, respectively) are detected (Fig. 4). These *in vivo* results show that the M23 peptidase domain Tal₉₀₁₋₁ is not involved in the proteolytic separation of the Tal protein N and C terminus.

The third mutant TP901-1 derivative, TP901-1erm_{Gly603*}, was designed to introduce a stop codon into the coding sequence of tal₉₀₁₋₁ at the position where it is known to undergo proteolysis. This mutation would be expected to result in a homogeneous population of phages, the reverse of TP901-1erm_{Gly>Arg}, with all of the Tal₉₀₁₋₁ proteins of the TP901-1erm phage population truncated at the sequence GGNSG*GG (position of stop codon highlighted by an asterisk). TP901-1erm_{Gly603*} also allows a comparison with mutant TP901-1erm_{H892A}, whose Tal protein is also expected to be incapable of degrading peptidoglycan. Western blots verified the truncated TP901-1erm_{Gly603*} protein (67.4 kDa), which runs slightly below its expected position on the SDS-PAGE gel (Fig. 4). As expected, no full-length Tal₉₀₁₋₁ protein (102.1 kDa) was detected in the Western blots of TP901-1erm_{Gly603*} in contrast TP901-1erm. Western blots using primary antibodies directed against the upper baseplate protein, BppU, which immediately succeeds tal₉₀₁₋₁, were performed on all mutants to verify that

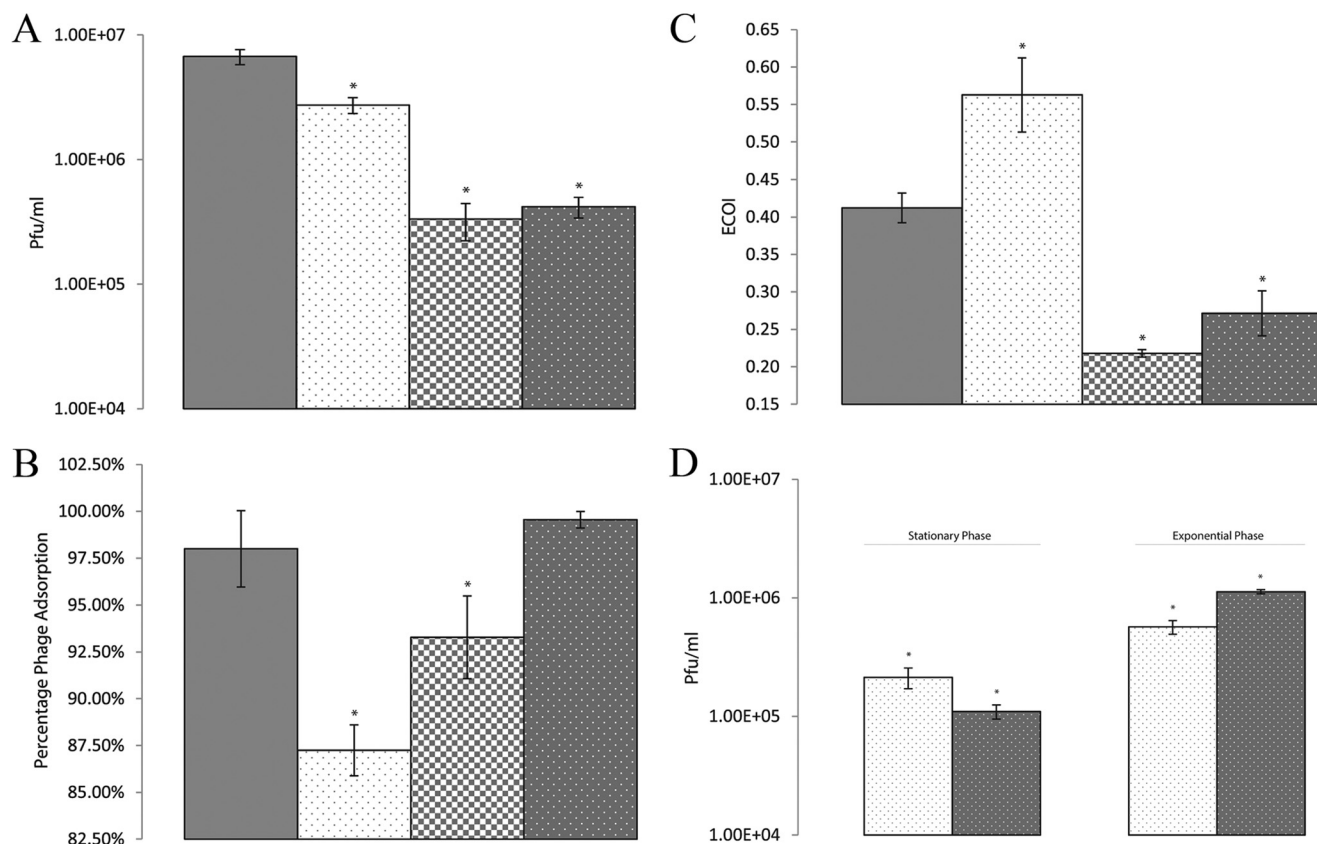


FIGURE 5. Bar graphs showing phage assays of TP901-1erm and mutant derivatives. TP901-1erm results are in solid gray, TP901-1erm_{Gly>Arg} are white with gray dots, TP901-1erm_{H892A} are gray with white checkers, and TP901-1erm_{Gly603*} are gray with white dots. Error bars indicate S.D., whereas asterisks indicate mutants that are statistical significance ($p < 0.05$). A, plaque assays of TP901-1erm and mutant derivatives. B, adsorption assays of TP901-1erm and mutant derivatives, measuring the percentage of bacterial bound phage in 10 min. C, ECOI formation by TP901-1erm and mutant derivatives. Each ECOI was calculated as the number of COIs formed on stationary phase cells relative to the number of COIs formed on exponentially growing cells. D, competition assays between TP901-1erm_{Gly>Arg} and TP901-1erm_{Gly603*}, comparing their ability to form COIs within 5 min. TP901-1erm_{Gly>Arg} are white with gray dots, and TP901-1erm_{Gly603*} are gray with white dots. Mutant phage TP901-1erm_{Gly>Arg} permanently retains the C terminus of its tail fiber protein, which possesses the 0, whereas mutant TP901-1erm_{Gly603*} incorporates only a truncated derivative of Tal₉₀₁₋₁.

there were no downstream effects caused by mutating *tal*₉₀₁₋₁ (results not shown).

Efficiency of Plaque Formation of TP901-1erm and Its Tal₉₀₁₋₁ Mutant Derivatives—To determine the effect of the various mutations of *tal*₉₀₁₋₁ on the efficiency of plaque formation of its corresponding TP901-1erm-derived phages, the ability of these mutant phages to infect lactococcal host 3107 was tested by plaque assay analysis. Plaque assays of TP901-1erm and its mutant derivatives were performed in triplicate on three independently produced lysates. The efficiencies of plaque formation of TP901-1erm_{Gly>Arg}, TP901-1erm_{H892A} and TP901-1erm_{Gly603*}, relative to TP901-1erm phage, were thus determined to be 0.408, 0.050, and 0.062, respectively (Fig. 5A). The plaque morphologies of the Tal₉₀₁₋₁ mutant phages were also noticeably different from those produced by wild type TP901-1erm: TP901-1erm_{Gly>Arg} produced plaques that were slightly smaller and hazier compared with TP901-1erm, whereas TP901-1erm_{H892A} and TP901-1erm_{Gly603*} both formed pinprick-sized plaques (results not shown).

Adsorption Assays of TP901-1 and Tal₉₀₁₋₁ Mutant Derivatives—Due to the location of Tal₉₀₁₋₁ in the TP901-1 virion, *i.e.* suspending directly below the host-recognizing baseplate organelle (26), we were curious about the effects of the Tal₉₀₁₋₁ mutations on adsorption. We therefore performed adsorption

assays on the TP901-1erm and its derived mutant phages and expressed the obtained data as the percentage of phages that bound to the bacterial host cells in 10 min (Fig. 5B). The multiplicity of infection for the adsorption assays, 0.01 phage per bacterial cell, was optimized based on conditions that yielded >95% of unmutated TP901-1erm adsorbing to its host *L. lactis* 3107 within 10 min (data not shown). The obtained phage adsorption efficiencies for the various phages were as follows: TP901-1erm, 98.01% ± 2.04%; TP901-1erm_{Gly>Arg}, 87.24% ± 1.36%; TP901-1erm_{H892A}, 93.28% ± 2.74%; and TP901-1erm_{Gly603*}, 99.56% ± 0.44%. These results demonstrate that mutants TP901-1erm_{Gly>Arg} and TP901-1erm_{H892A} significantly differ in their host adsorption efficiencies compared with TP901-1 ($p < 0.05$), whereas mutant TP901-1_{Gly603*} does not (Fig. 5B).

Efficiency of Formation of Centers of Infection—The M23 peptidase domain associated with Tal₂₀₀₉ and Tal₉₀₁₋₁ is expected to facilitate cell wall penetration and genome delivery, particularly during conditions where the cell wall is extensively cross-linked, as would be expected for stationary phase cells (8, 54). To compare the ability of TP901-1erm and mutant derivatives to infect stationary phase cells compared with exponentially growing cells, the phage ECOIs were calculated (see “Materials and Methods”). The ECOI for TP901-1erm was cal-

Tail-associated Lytic Enzymes of Siphoviridae Phages

culated as 0.41 ± 0.02 , TP901-1 $erm_{Gly>Arg}$ as 0.56 ± 0.05 , TP901-1 erm_{H892A} as 0.22 ± 0.005 and TP901-1 erm_{Gly603}^* as 0.27 ± 0.03 . The difference in the abilities of the mutant phage to infect stationary phase cells, relative to TP901-1 erm , is considered to be statistically significant ($p < 0.05$; Fig. 5C).

Competition Assays between TP901-1 Mutants with and without Tail Fiber—To compare and contrast the biological significance of TP901-1 proteolytic processing of Tal₉₀₁₋₁, the TP901-1 mutants permanently possessing or lacking the tail fiber were mixed together and simultaneously allowed to infect. The number of COIs established could be calculated due to distinguishing plaque morphologies formed by these phages. TP901-1 $erm_{Gly>Arg}$, which possesses the C terminus of Tal₉₀₁₋₁ and thus the M23 peptidase domain, forms more COIs in stationary phase cells than TP901-1 erm_{Gly603}^* . In contrast, TP901-1 erm_{Gly603}^* , which lacks the C terminus of the tail fiber and the PGH motif, is more efficient at establishing COIs in exponentially growing cells (Fig. 5D).

DISCUSSION

The proteolysis of Tuc2009 and TP901-1 Tal protein represents a molecular “hedge betting” mechanism to produce a naturally mixed population of phages, which are simultaneously adapted for efficient host adsorption and host penetration. Many phages have evolved sophisticated strategies to efficiently infect their hosts; however, to our knowledge, the proteolytic processing step of Tal₂₀₀₉ and Tal₉₀₁₋₁ represents a novel phage mechanism for infection optimization under particular conditions.

Not all phages appear to require PGH domains to facilitate host penetration and infection, as many phages lack any recognizable PGH domain associated with their structural proteins. However, there is growing evidence to support that virion-associated PGH domains facilitate infection under conditions where the cell wall is extensively cross-linked (for a recent review, see Ref. 55). In the current study, we show that the M23 peptidase of Tal₂₀₀₉ possesses a D-Ala-D-Asp endopeptidase specificity. This tail-associated lytic activity facilitates phage infection by undoing the interpeptide cross-linkage of peptidoglycan glycan strands. As the majority of the sequenced P335 species lactococcal phages possess PGH domains associated with their tail proteins, the localized degradation of the bacterial cell wall is predicted to be an important step in the initial stages of infection by this species of phage.

In this study, we clearly show that TP901-1 erm -derived mutants defective in their tail-associated PGH activity are not completely deficient in phage infection but display decreased infection efficiencies. This is consistent with the study of Moak and colleagues (56), who demonstrated that mutagenesis of the virion-associated PGH domain of T7 did not inhibit but merely delayed infection. Furthermore, the reduced ability of TP901-1 erm PGH mutants to infect stationary phase cells is in agreement with the study of Puri *et al.* (8), where the lytic domain of the tail fiber of *Mycobacterium* phage TM4 was necessary for efficient infection of stationary phase cells.

It was previously reported by Scholl and colleagues (57) that phage K1-5 encodes and incorporates two different tail fiber proteins into its virion, adapting the phage to penetrating hosts

with a different cell envelope composition. Phages Tuc2009 and TP901-1 (and perhaps many other phages) have similarly evolved a novel strategy to generate a heterogeneous population. Through Tal proteolysis, the lactococcal phages Tuc2009 and TP901-1 generate two phage types: incorporating either a truncated Tal protein or incorporating a full-length tail fiber with an associated lytic domain. Phages that feature a PGH domain in their virion are better adapted to infecting bacteria with a higher degree of cross-linkage in their cell wall. However, this evolutionary advantage appears to be a double-edged sword, as the fitness cost is at the expense of phage adsorption efficiency.

The study of lactococcal phages pertains not only to their industrial significance but their broader importance as model systems. The clear differences in the tail fibers and infection mechanisms of lactococcal phages show the multifaceted approach by phages to achieve infection. Studies characterizing these underlying molecular processes serve to better understand Siphoviridae, and their host interactions, in the biosphere.

REFERENCES

1. Ackermann, H. W. (2007) 5500 Phages examined in the electron microscope. *Arch. Virol.* **152**, 227–243
2. Wommack, K. E., and Colwell, R. R. (2000) Virioplankton: viruses in aquatic ecosystems. *Microbiol. Mol. Biol. Rev.* **64**, 69–114
3. Katsura, I., and Kühn, P. W. (1975) Morphogenesis of the tail of bacteriophage λ . III. Morphogenetic pathway. *J. Mol. Biol.* **91**, 257–273
4. Vegge, C. S., Brøndsted, L., Neve, H., Mc Grath, S., van Sinderen, D., and Vogensen, F. K. (2005) Structural characterization and assembly of the distal tail structure of the temperate lactococcal bacteriophage TP901-1. *J. Bacteriol.* **187**, 4187–4197
5. Berkane, E., Orlik, F., Stegmeier, J. F., Charbit, A., Winterhalter, M., and Benz, R. (2006) Interaction of bacteriophage λ with its cell surface receptor: an *in vitro* study of binding of the viral tail protein gpI to LamB (Maltoporin). *Biochemistry* **45**, 2708–2720
6. Duplessis, M., and Moineau, S. (2001) Identification of a genetic determinant responsible for host specificity in *Streptococcus thermophilus* bacteriophages. *Mol. Microbiol.* **41**, 325–336
7. Jakutyte, L., Lurz, R., Baptista, C., Carballido-Lopez, R., São-José, C., Tavares, P., and Daugelavičius, R. (2012) First steps of bacteriophage SPP1 entry into *Bacillus subtilis*. *Virology* **422**, 425–434
8. Puri, M., and Hatfull, G. F. (2006) A peptidoglycan hydrolase motif within the mycobacteriophage TM4 tape measure protein promotes efficient infection of stationary phase cells. *Mol. Microbiol.* **62**, 1569–1585
9. Boulanger, P., Jacquot, P., Plançon, L., Chami, M., Engel, A., Parquet, C., Herbeuval, C., and Letellier, L. (2008) Phage T5 straight tail fiber is a multifunctional protein acting as a tape measure and carrying fusogenic and muralytic activities. *J. Biol. Chem.* **283**, 13556–13564
10. Roessner, C. A., and Ihler, G. M. (1986) Formation of transmembrane channels in liposomes during injection of λ DNA. *J. Biol. Chem.* **261**, 386–390
11. Plisson, C., White, H. E., Auzat, I., Zafarani, A., São-José, C., Lhuillier, S., Tavares, P., and Orlova, E. V. (2007) Structure of bacteriophage SPP1 tail reveals trigger for DNA ejection. *EMBO J.* **26**, 3720–3728
12. Gurnev, P. A., Oppenheim, A. B., Winterhalter, M., and Bezrukov, S. M. (2006) Docking of a single phage λ to its membrane receptor maltoporin as a time-resolved event. *J. Mol. Biol.* **359**, 1447–1455
13. Roessner, C. A., Struck, D. K., and Ihler, G. M. (1983) Morphology of complexes formed between bacteriophage λ and structures containing the λ receptor. *J. Bacteriol.* **153**, 1528–1534
14. Roessner, C. A., and Ihler, G. M. (1984) Proteinase sensitivity of bacteriophage λ tail proteins gpI and pH in complexes with the λ receptor. *Journal of Bacteriology* **157**, 165–170

15. Feucht, A., Schmid, A., Benz, R., Schwarz, H., and Heller, K. J. (1990) Pore formation associated with the tail-tip protein pb2 of bacteriophage T5. *J. Biol. Chem.* **265**, 18561–18567
16. Kleerebezem, M., Beerthuyzen, M. M., Vaughan, E. E., de Vos, W. M., and Kuipers, O. P. (1997) Controlled gene expression systems for lactic acid bacteria: transferable nisin-inducible expression cassettes for *Lactococcus*, *Leuconostoc*, and *Lactobacillus* spp. *Appl. Environ. Microbiol.* **63**, 4581–4584
17. Böhm, J., Lambert, O., Frangakis, A. S., Letellier, L., Baumeister, W., and Rigaud, J. L. (2001) FhuA-mediated phage genome transfer into liposomes: a cryo-electron tomography study. *Curr. Biol.* **11**, 1168–1175
18. Goulet, A., Lai-Kee-Him, J., Veessler, D., Auzat, I., Robin, G., Shepherd, D. A., Ashcroft, A. E., Richard, E., Lichière, J., Tavares, P., Cambillau, C., and Bron, P. (2011) The opening of the SPP1 bacteriophage tail, a prevalent mechanism in Gram-positive-infecting siphophages. *J. Biol. Chem.* **286**, 25397–25405
19. São-José, C., Baptista, C., and Santos, M. A. (2004) *Bacillus subtilis* operon encoding a membrane receptor for bacteriophage SPP1. *J. Bacteriol.* **186**, 8337–8346
20. São-José, C., Lhuillier, S., Lurz, R., Melki, R., Lepault, J., Santos, M. A., and Tavares, P. (2006) The ectodomain of the viral receptor YueB forms a fiber that triggers ejection of bacteriophage SPP1 DNA. *J. Biol. Chem.* **281**, 11464–11470
21. Baptista, C., Santos, M. A., and São-José, C. (2008) Phage SPP1 reversible adsorption to *Bacillus subtilis* cell wall teichoic acids accelerates virus recognition of membrane receptor YueB. *J. Bacteriol.* **190**, 4989–4996
22. Garneau, J. E., and Moineau, S. (2011) Bacteriophages of lactic acid bacteria and their impact on milk fermentations. *Microb. Cell Fact.* **10**, S20
23. Deveau, H., Labrie, S. J., Chopin, M. C., and Moineau, S. (2006) Biodiversity and classification of lactococcal phages. *Appl. Environ. Microbiol.* **72**, 4338–4346
24. Mahony, J., Murphy, J., and van Sinderen, D. (2012) Lactococcal 936-type phages and dairy fermentation problems: from detection to evolution and prevention. *Front. Microbiol.* **3**, 335
25. Veessler, D., and Cambillau, C. (2011) A common evolutionary origin for tailed-bacteriophage functional modules and bacterial machineries. *Microbiol. Mol. Biol. Rev.* **75**, 423–433
26. Bebeacua, C., Bron, P., Lai, L., Vegge, C. S., Brøndsted, L., Spinelli, S., Campanacci, V., Veessler, D., van Heel, M., and Cambillau, C. (2010) Structure and molecular assignment of lactococcal phage TP901-1 baseplate. *J. Biol. Chem.* **285**, 39079–39086
27. Johnsen, M. G., Neve, H., Vogensen, F. K., and Hammer, K. (1995) Virion positions and relationships of lactococcal temperate bacteriophage TP901-1 proteins. *Virology* **212**, 595–606
28. Campanacci, V., Veessler, D., Lichière, J., Blangy, S., Sciara, G., Moineau, S., van Sinderen, D., Bron, P., and Cambillau, C. (2010) Solution and electron microscopy characterization of lactococcal phage baseplates expressed in *Escherichia coli*. *J. Struct. Biol.* **172**, 75–84
29. Bebeacua, C., Lai, L., Vegge, C. S., Brøndsted, L., van Heel, M., Veessler, D., and Cambillau, C. (2012) Visualizing a Complete Siphoviridae by Single-particle Electron Microscopy: The Structure of Lactococcal Phage TP901-1. *J. Virol.* **87**, 1061–1068
30. Veessler, D., Robin, G., Lichière, J., Auzat, I., Tavares, P., Bron, P., Campanacci, V., and Cambillau, C. (2010) Crystal structure of bacteriophage SPP1 distal tail protein (gp19.1): a baseplate hub paradigm in gram-positive infecting phages. *J. Biol. Chem.* **285**, 36666–36673
31. Kenny, J. G., McGrath, S., Fitzgerald, G. F., and van Sinderen, D. (2004) Bacteriophage Tuc2009 encodes a tail-associated cell wall-degrading activity. *J. Bacteriol.* **186**, 3480–3491
32. van Pijkeren, J. P., and Britton, R. A. (2012) High efficiency recombineering in lactic acid bacteria. *Nucleic Acids Res.* **40**, e76
33. Van Pijkeren, J. P., Neoh, K. M., Sirias, D., Findley, A. S., and Britton, R. A. (2012) Exploring optimization parameters to increase ssDNA recombineering in *Lactococcus lactis* and *Lactobacillus reuteri*. *Bioengineered* **3**, 209–217
34. Seegers, J. F., Mc Grath, S., O'Connell-Motherway, M., Arendt, E. K., van de Guchte, M., Creaven, M., Fitzgerald, G. F., and van Sinderen, D. (2004) Molecular and transcriptional analysis of the temperate lactococcal bacteriophage Tuc2009. *Virology* **329**, 40–52
35. Arendt, E. K., Daly, C., Fitzgerald, G. F., and van de Guchte, M. (1994) Molecular characterization of lactococcal bacteriophage Tuc2009 and identification and analysis of genes encoding lysin, a putative holin, and two structural proteins. *Appl. Environ. Microbiol.* **60**, 1875–1883
36. Kuipers, O., de Ruyter, P. G. G. A., Kleerebezem, M., and de Vos, W. M. (1998) Quorum sensing-controlled gene expression in lactic acid bacteria. *J. Biotechnol.* **64**, 15–21
37. Courtin, P., Miranda, G., Guillot, A., Wessner, F., Mézange, C., Domakova, E., Kulakauskas, S., and Chapot-Chartier, M. P. (2006) Peptidoglycan structure analysis of *Lactococcus lactis* reveals the presence of an L,D-carboxypeptidase involved in peptidoglycan maturation. *J. Bacteriol.* **188**, 5293–5298
38. Lillehaug, D. (1997) An improved plaque assay for poor plaque-producing temperate lactococcal bacteriophages. *J. Appl. Microbiol.* **83**, 85–90
39. Sanders, M. E., and Klaenhammer, T. R. (1980) Restriction and modification in group N streptococci: effect of heat on development of modified lytic bacteriophage. *Appl. Environ. Microbiol.* **40**, 500–506
40. Moineau, S., Durmaz, E., Pandian, S., and Klaenhammer, T. R. (1993) Differentiation of Two Abortive Mechanisms by Using Monoclonal Antibodies Directed toward Lactococcal Bacteriophage Capsid Proteins. *Appl. Environ. Microbiol.* **59**, 208–212
41. Mc Grath, S., Neve, H., Seegers, J. F., Eijlander, R., Vegge, C. S., Brøndsted, L., Heller, K. J., Fitzgerald, G. F., Vogensen, F. K., and van Sinderen, D. (2006) Anatomy of a lactococcal phage tail. *J. Bacteriol.* **188**, 3972–3982
42. Donovan, D. M., Dong, S., Garrett, W., Rousseau, G. M., Moineau, S., and Pritchard, D. G. (2006) Peptidoglycan hydrolase fusions maintain their parental specificities. *Appl. Environ. Microbiol.* **72**, 2988–2996
43. Loessner, M. J., Kramer, K., Ebel, F., and Scherer, S. (2002) C-terminal domains of *Listeria monocytogenes* bacteriophage murein hydrolases determine specific recognition and high-affinity binding to bacterial cell wall carbohydrates. *Mol. Microbiol.* **44**, 335–349
44. Sass, P., and Bierbaum, G. (2007) Lytic activity of recombinant bacteriophage phi11 and phi12 endolysins on whole cells and biofilms of *Staphylococcus aureus*. *Appl. Environ. Microbiol.* **73**, 347–352
45. Sudiarta, I. P., Fukushima, T., and Sekiguchi, J. (2010) *Bacillus subtilis* CwlP of the SP- β prophage has two novel peptidoglycan hydrolase domains, muramidase and cross-linkage digesting DD-endopeptidase. *J. Biol. Chem.* **285**, 41232–41243
46. Odintsov, S. G., Sabala, I., Marcyjaniak, M., and Bochtler, M. (2004) Latent LytM at 1.3 Å resolution. *J. Mol. Biol.* **335**, 775–785
47. Spencer, J., Murphy, L. M., Conners, R., Sessions, R. B., and Gamblin, S. J. (2010) Crystal structure of the LasA virulence factor from *Pseudomonas aeruginosa*: substrate specificity and mechanism of M23 metallopeptidases. *J. Mol. Biol.* **396**, 908–923
48. Pedersen, M., Ostergaard, S., Bresciani, J., and Vogensen, F. K. (2000) Mutational analysis of two structural genes of the temperate lactococcal bacteriophage TP901-1 involved in tail length determination and baseplate assembly. *Virology* **276**, 315–328
49. Vegge, C. S., Neve, H., Brøndsted, L., Heller, K. J., and Vogensen, F. K. (2006) Analysis of the collar-whisker structure of temperate lactococcal bacteriophage TP901-1. *Appl. Environ. Microbiol.* **72**, 6815–6818
50. Vegge, C. S., Vogensen, F. K., Mc Grath, S., Neve, H., van Sinderen, D., and Brøndsted, L. (2006) Identification of the lower baseplate protein as the antireceptor of the temperate lactococcal bacteriophages TP901-1 and Tuc2009. *J. Bacteriol.* **188**, 55–63
51. Law, J., Buist, G., Haandrikman, A., Kok, J., Venema, G., and Leenhouts, K. (1995) A system to generate chromosomal mutations in *Lactococcus lactis* which allows fast analysis of targeted genes. *J. Bacteriol.* **177**, 7011–7018
52. Christiansen, B., Johnsen, M. G., Stenby, E., Vogensen, F. K., and Hammer, K. (1994) Characterization of the lactococcal temperate phage TP901-1 and its site-specific integration. *J. Bacteriol.* **176**, 1069–1076
53. Hooper, N. M. (1994) Families of zinc metalloproteases. *FEBS Lett.* **354**, 1–6
54. Vollmer, W., Blanot, D., and de Pedro, M. A. (2008) Peptidoglycan structure and architecture. *FEMS Microbiol. Rev.* **32**, 149–167
55. Rodriguez-Rubio, L., Martinez, B., Donovan, D. M., Rodriguez, A., and Garcia, P. (2012) *Crit. Rev. Microbiol.* [Epub ahead of print]

Tail-associated Lytic Enzymes of Siphoviridae Phages

56. Moak, M., and Molineux, I. J. (2000) Role of the Gp16 lytic transglycosylase motif in bacteriophage T7 virions at the initiation of infection. *Mol. Microbiol.* **37**, 345–355
57. Scholl, D., Rogers, S., Adhya, S., and Merrill, C. R. (2001) Bacteriophage K1-5 encodes two different tail fiber proteins, allowing it to infect and replicate on both K1 and K5 strains of *Escherichia coli*. *J. Virol.* **75**, 2509–2515
58. Wegmann, U., O'Connell-Motherway, M., Zomer, A., Buist, G., Shearman, C., Canchaya, C., Ventura, M., Goesmann, A., Gasson, M. J., Kuipers, O. P., van Sinderen, D., and Kok, J. (2007) Complete genome sequence of the prototype lactic acid bacterium *Lactococcus lactis* subsp. *cremoris* MG1363. *J. Bacteriol.* **189**, 3256–3270
59. Koch, B., Christiansen, B., Evison, T., Vogensen, F. K., and Hammer, K. (1997) Construction of specific erythromycin resistance mutations in the temperate lactococcal bacteriophage TP901-1 and their use in studies of phage biology. *Appl. Environ. Microbiol.* **63**, 2439–2441
60. Braun, V., Hertwig, S., Neve, H., Geis, A., and Teuber, T. (1989) Taxonomic Differentiation of Bacteriophages of *Lactococcus lactis* by Electron Microscopy, DNA-DNA Hybridization, and Protein Profiles. *Microbiology* **135**, 2551–2560
61. de Ruyter, P. G., Kuipers, O. P., and de Vos, W. M. (1996) Controlled gene expression systems for *Lactococcus lactis* with the food-grade inducer nisin. *Appl. Environ. Microbiol.* **62**, 3662–3667
62. Costello, V. A. (1988) Characterization of bacteriophage-host interactions in *Streptococcus cremoris* UC503 and related lactic streptococci. Ph.D thesis, National University of Ireland, University College Cork, Ireland
63. Kuipers, O. P., Beerthuyzen, M. M., Siezen, R. J., and De Vos, W. M. (1993) Characterization of the nisin gene cluster nisABTCIPR of *Lactococcus lactis*. Requirement of expression of the nisA and nisI genes for development of immunity. *Eur. J. Biochem.* **216**, 281–291

The Lactococcal Phages Tuc2009 and TP901-1 Incorporate Two Alternate Forms of Their Tail Fiber into Their Virions for Infection Specialization

Stephen R. Stockdale, Jennifer Mahony, Pascal Courtin, Marie-Pierre Chapot-Chartier, Jan-Peter van Pijkeren, Robert A. Britton, Horst Neve, Knut J. Heller, Bashir Aideh, Finn K. Vogensen and Douwe van Sinderen

J. Biol. Chem. 2013, 288:5581-5590.

doi: 10.1074/jbc.M112.444901 originally published online January 8, 2013

Access the most updated version of this article at doi: [10.1074/jbc.M112.444901](https://doi.org/10.1074/jbc.M112.444901)

Alerts:

- [When this article is cited](#)
- [When a correction for this article is posted](#)

[Click here](#) to choose from all of JBC's e-mail alerts

Supplemental material:

<http://www.jbc.org/content/suppl/2013/01/08/M112.444901.DC1>

This article cites 61 references, 33 of which can be accessed free at <http://www.jbc.org/content/288/8/5581.full.html#ref-list-1>